Chemistry and Physics of Lipids 223 (2019) 104791

Contents lists available at ScienceDirect

Chemistry and Physics of Lipids

journal homepage: www.elsevier.com/locate/chemphyslip

Self-assembled systems based on novel hydroxyethylated imidazolium-containing amphiphiles: Interaction with DNA decamer, protein and lipid

Darya A. Kuznetsova, Dinar R. Gabdrakhmanov*, Svetlana S. Lukashenko, Alexandra D. Voloshina, Anastasiia S. Sapunova, Ruslan R. Kashapov, Lucia Ya. Zakharova

Arbuzov Institute of Organic and Physical Chemistry, FRC Kazan Scientific Center of RAS, Arbuzov str. 8, Kazan, Russian Federation

ARTICLE INFO

Keywords:
Cationic surfactant
Lipoplex
Oligonucleotide
Nonviral vectors
Lipid
Temperature of phase transition
Protein
Bovine serum albumin

ABSTRACT

The study on aggregation capacity of novel imidazolium-containing amphiphiles of 1-(2-hydroxyethyl)alkylimidazolium bromide series and their interaction with bio-objects (DNA decamer, bovine serum albumin, phospholipid) was performed. It was revealed that introduction of hydroxyethyl moiety into the surfactant molecule resulted in 1.5–2-fold decrease of critical micelle concentration. These modified amphiphiles quantitatively bind DNA decamer due to intercalation and hydrophobic interactions with lipoplex formation. The evaluation of membranotropic properties of these surfactants exhibited that initiation of disordering and compression of the model cell wall consisting of dipalmitoyl phosphocholine (regulation of permeability for various compounds) could be achieved by variation of the length of hydrophobic tail of imidazolium-containing amphiphiles. Transition from individual surfactants solutions to their mixtures with protein (bovine serum albumin) is accompanied by 8-fold decrease of aggregation thresholds and characterized by the presence of two critical points. The binding of components of surfactant/BSA binary systems took place through tryptophan amino acid residue of peptide macromolecule.

1. Introduction

Nowadays, the application of cationic surfactants concerns biotechnologies in virtually all branches of industry. For example, it is well-known that amphiphiles bearing positive charge are essential components of detergents (Baker et al., 2004), capable to act as micellar catalysts (Gabdrakhmanov et al., 2015b; 2016a, 2016b; Samarkina et al., 2016, 2017c), nanocontainers for molecules of interest (Gabdrakhmanov et al., 2016c; Mandal et al., 2014; Samarkina et al., 2017a; Yan et al., 2015), microemulsions for drug delivery (Kaur et al., 2018; Mirgorodskaya et al., 2017, 2018), and nonviral vectors (Gabdrakhmanov et al., 2015a; Kumar et al., 2004; Zhou et al., 2013). They also exhibit antimicrobial activities (Kashapov et al., 2019) and could be used to fabricate complexes with proteins (Gabdrakhmanov et al., 2018; Misra et al., 2015; Samarkina et al., 2017b, 2019; Vasilieva et al., 2018b; Zheng et al., 2017) and form modified liposomes (Bombelli et al., 2010; Koirala et al., 2016; Kuznetsova et al., 2019a, 2019b; Pashirova et al., 2018).

From this viewpoint the amphiphiles bearing imidazolium head group are attractive candidates for abovementioned applications. These compounds are often considered as room temperature ionic liquids and were thoroughly investigated (Benedetto and Ballone, 2016; Benedetto, 2017; Wang et al., 2018; Benedetto and Ballone, 2018), in particular, in terms of their capability to interact with important biomolecules: i) they are able to form complex with nucleic acids through their backbone and groove binding; therefore could act as a chemical DNA stabilizer and nuclease inhibitor (Tateishi-Karimata and Sugimoto, 2018); ii) their influence on protein structure is double-natured and may induce both unfolding and folding of polypeptide macromolecule, e.g. human serum albumin under various external conditions (Nandi and Bhattacharyya, 2018); iii) the imidazolium-based compounds tend to change physico-chemical parameters of lipid bilayers. The latter is of great importance and should be considered separately, since regulation of these properties is a key factor for delivery of desired compounds into the cell through its membrane. Depending on the nature of lipid bilayer, these compounds could exhibit stabilization or destructing effect on model cell membrane (Kumar et al., 2018). It was shown, that the length of hydrophobic tail of imidazolium-based amphiphile have dramatic effect on fluidity, which increases significantly with tail elongation due to the higher disordering effect (Benedetto and Ballone, 2016; Benedetto, 2017; Benedetto and Ballone, 2018). This phenomenon is responsible for the increase in permeability of lipid bilayer (Lim

* Corresponding author.
E-mail address: nemezc1988@yandex.ru (D.R. Gabdrakhmanov).

https://doi.org/10.1016/j.chemphyslip.2019.104791
Received 8 May 2019; Received in revised form 30 June 2019; Accepted 14 July 2019
Available online 18 July 2019

et al., 2015; Kumar et al., 2018) and can be used as a perspective tool to improve the cellular uptake of active compounds, e.g. drug. Nevertheless, it should be noted that the majority of investigations focus on the imidazolium derivatives with alkyl tails up to tetradecyl derivatives, and do not consider the higher homologues.

Along with the substitution of ammonium head group by imidazolium one, there are other attractive techniques for modification of amphiphile molecules directed at the improvement of its practically useful properties. One of them is the introduction of hydroxyalkyl groups in the surfactant structure. This modification is responsible for the improvement of surfactant aggregation characteristics and functional activity (Asadov et al., 2019; Chauhan et al., 2014; Liu et al., 2015; Vasilieva et al., 2018a; Yackevich et al., 2014). In particular, the amphiphilic compounds bearing hexadecyl hydrophobic tail demonstrate superior bactericide and bacteriostatic activity against gram-positive bacteria as compared to those without hydroxyl group and conventional cationic amphiphile cetyltrimethylammonium bromide (Vasilieva et al., 2018a). Similar increase of antimicrobial activity also occurs in the case of amphiphile of ammonium series modified with the hydroxyethyl moiety: this amphiphilic compound stopped the growth of *Staphylococcus aureus* and *Candida albicans* bacteria even at low concentrations (Asadov et al., 2019). Transition from hydroxyalkylated ammonium surfactants to imidazolium ones may be considered as perspective way to obtain low-cytotoxic (Aggarwal and Singh, 2018) and effective antimicrobial agents against several strains (Kuznetsova et al., 2019b). For example, functionalized hexyl derivatives are equivalent to unfunctionalized dodecyl ones in terms of their activity toward *Staphylococcus aureus* (Albalawi et al., 2018; Demberelnyamba et al., 2004). It could be noted that for both types of amphiphiles an increase of antibacterial effect with elongation of hydrophobic tail is observed; however, this effect reaches its maximum in the case of dodecyl- or tetradecyl derivative and further don't increase (Demberelnyamba et al., 2004; Zheng et al., 2016). The presence of hydroxyethyl fragments in the surfactant molecule may affect significantly the complexation with biomolecules like bovine serum albumin (BSA) and human serum albumin. The conventional mechanism of component interaction in these systems regards electrostatic attraction and hydrophobic interactions (Parray et al., 2018; Xie et al., 2016). Introduction of OH-group to the amphiphile structure strengthens the additional hydrogen bonding interactions (Sinha et al., 2016; Qin et al., 2015). For example, the presence of OH-group significantly increases electrostatic interactions with BSA in the case of conventional cationic amphiphiles of trimethylammonium series with alkyl chains from tetradecyl to octadecyl derivative (Xie et al., 2016), while for amphiphile with dodecyl tail the hydrogen bonding takes place (Qin et al., 2015).

In the framework of this report we suggest to combine two above-mentioned well-proven approaches for construction of novel multifunctional amphiphilic building blocks and fill the gap of undescribed high homologues. Therefore, this study was dedicated to the estimation of aggregation characteristics and functional activity of imidazolium-containing amphiphiles bearing various hydrophobic tails (14, 16 and 18 carbon atoms) and hydroxyethyl moieties (Fig. 1, IA-n(OH)). In particular, biotechnological potential of these amphiphiles were tested in interaction with DNA decamer, protein (bovine serum albumin) and model lipid bilayer composed of 1,2-dipalmitoyl-*sn*-glycero-3-phosphocholine (DPPC).

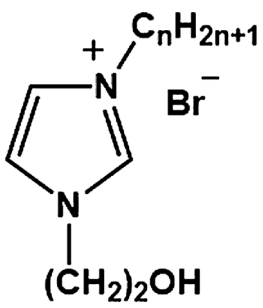

Fig. 1. Chemical structure of IA-n(OH) (n = 14,16,18).

2. Experimental section

2.1. Materials, preparation of solutions and dispersions

2.1.1. Materials

1,2-dipalmitoyl-*sn*-glycero-3-phosphocholine (DPPC, Sigma-Aldrich, 99%), bovine serum albumin (Sigma-Aldrich, 99%), ethidium bromide (EB) (Sigma-Aldrich, 95%), Orange OT (Sigma-Aldrich; 95%), metronidazole (Sigma-Aldrich, 99%) were used as received. DNA decamer (oligonucleotide, ONu) consisting of ten base pairs, strand 2 (GCGTTAACGC, molecular weight 3028) was purchased from Joint Stock Company Syntol (Moscow, Russia).

2.1.2. Preparation of samples

Sample solutions were prepared in deionized water (18.2 MΩ) obtained from a Millipore Direct-Q 5 UV water purification system.

Liposomes preparation was carried out by thin lipid hydration technique as follows: 5.4 mg of DPPC powder was dissolved in 100 μL of chloroform. The solvent was evaporated overnight at the room temperature. The resulting lipid film was suspended by 1 mL of water and thermostated at 55–60 °C on water bath during 30 min. The rude suspension obtained was frozen and thawed 5 times using liquid nitrogen and water bath (60 °C), respectively. After that dispersion was extruded at least 20 times by using a syringe extruder (LiposoFast Basic, Avestin, Ottawa) through a polycarbonate filter with 100-nm pores. Preparation of liposome for metronidazole entrapment was performed in similar way by dissolving required amount of drug (20 mM) in the mixture with lipid and amphiphile in chloroform.

The phosphate buffer (pH 6.9) was used for preparation of solutions containing BSA.

The DNA decamer stock solution was prepared in 4 mM tris-HCl buffer (pH 8.0) and diluted to 10 mM (concentration per nucleotide unit). The mixture was heated at 95 °C for 5 min and immediately chilled down in the ice bath.

2.1.3. Synthesis of homologous series of imidazolium-containing amphiphiles

1-(2-hydroxyethyl)tetradecylimidazolium bromide. The mixture containing 1.0 g (8.9 mmol) of 1-(2-hydroxyethyl)imidazole and 2.72 g (9.8 mmol) of 1-tetradecylbromide dissolved in 10 mL of acetonitrile was boiled with reflux condenser for 24 h. The precipitate formed during cooling was filtered, purified by recrystallization from ethyl acetate and dried under vacuum. Yield: 2.70 g (73%). Mp = 40–42 °C. IR-spectrum (KBr), cm^{-1}: 3532, 3330, 3134, 3069, 2917, 2850, 1564, 1472, 1379, 1165,1071, 873, 792, 720. ^{1}H NMR spectrum, 400 MHz ($CDCl_3$), δ, ppm, *J*/Hz: 0.87 t (3H, *J* = 6.8), 1.25–1.33 m (22 H), 1.87–1.91 m (2 H), 3.98 t (2H, *J* = 4.9), 4.26 t (2H, *J* = 7.5), 4.53 t (2H, *J* = 4.9), 7.31 s (1 H), 7.63 s (1 H), 9.73 s (1 H). ESI MS, *m/z*: 309.5 $[M\text{-}Br]^+$. Calculated, %: $C_{19}H_{37}N_2OBr$: C 58.60; H 9.57; N 7.19; Br 20.52; found, %: C 58.02; H 10.05; N 7.21; Br 19.99.

1-(2-hydroxyethyl)hexadecylimidazolium bromide. The mixture containing 1.0 g (8.9 mmol) of 1-(2-hydroxyethyl)imidazole and 2.99 g (9.8 mmol) of 1-hexadecylbromide dissolved in 10 mL of acetonitrile was boiled with reflux condenser for 24 h. The precipitate formed during cooling was filtered, purified by recrystallization from ethyl acetate and dried under vacuum. Yield: 2.25 g (58%). Mp = 52–54 °C. IR-spectrum (KBr), cm^{-1}: 3532, 3330, 3134, 3069, 2917, 2850, 1564, 1472, 1379, 1165,1071, 873, 792, 720. ^{1}H NMR spectrum, 400 MHz ($CDCl_3$), δ, ppm, *J*/Hz: 0.88 t (3H, *J* = 6.8), 1.25–1.33 m (26 H), 1.91 m (2 H), 3.98 t (2H, *J* = 4.91), 4.26 t (2H, *J* = 7.64), 4.53 t (2H, *J* = 7.90), 7.31 d (1 H), 7.63 d (1 H), 9.73 s (1 H). ESI MS, *m/z*: 337.6$[M\text{-}Br]^+$.

Calculated, %: $C_{21}H_{41}N_2OBr$: C 60.42; H 9.89; N 6.71; Br 19.14; found, %: C 60.23; H 10.12; N 6.45; Br 19.07.

1-(2-hydroxyethyl)octadecylimidazolium bromide. The mixture containing 1.0 g (8.9 mmol) of 1-(2-hydroxyethyl)imidazole and 3.59 g (9.8 mmol) of 1-octadecylbromide dissolved in 10 mL of acetonitrile was boiled with reflux condenser for 24 h. The precipitate formed during cooling was filtered, purified by recrystallization from ethyl acetate and dried under vacuum. Yield: 3.00 g (69%). Mp = 56–58 °C. IR-spectrum (KBr), cm^{-1}: 3325, 3140, 3080, 2915, 2850, 1565, 1472, 1378, 1165,1071, 871, 721. ^{1}H NMR spectrum, 400 MHz ($CDCl_3$), δ, ppm, *J*/Hz: 0.87 t (3H, *J* = 7.0), 1.24–1.32 m (30 H), 1.89–1.92 m (2 H), 3.98 t (2H, *J* = 4.27), 4.26 t (2H, *J* = 7.6), 4.53 t (2H, *J* = 4.90), 7.31 s (1 H), 7.63 s (1 H), 9.73 s (1 H). ESI MS, *m/z*: 365.5 $[M\text{-}Br]^+$. Calculated, %: $C_{23}H_{45}$ N_2 OBr: C 62.00; H 10.18; N 6.29; Br 17.93; found, %: C 61.75; H 10.43; N 6.22; Br 17.58.

2.2. Methods

2.2.1. Tensiometry

A Krűss K06 tensiometer (Du Nouy ring detachment method) was used for measurements of surface tension (Samarkina et al., 2017a). The volume of amphiphiles solutions was 10 mL. Each measurement was repeated at least 3 times, and the measurements with deviation between them ≤ 1 mN/m were taken in account. The ring was soaked in ethanol and dried between measurements. In the case of amphiphile/BSA binary systems the samples were equilibrated for 3 min at room temperature before each measurement.

2.2.2. Fluorescence spectroscopy

Emission spectra were measured using a Cary Eclipse G9800A fluorescence spectrophotometer. Fluorescence spectra of oligonucleotide-EB complexes were recorded in the range of 500–700 nm (excitation wavelength was 480 nm). A 0.8 mL sample containing 0.5 μM of EB and 10 mM concentration of oligonucleotide (counting on 1 base pair) in 4 mM tris-HCl buffer (pH 8.0) was equilibrated for 10 min at 25 °C. After that, a certain amount of the amphiphile solution was added into the mixture and the fluorescence emission spectrum was recorded (Mirgorodskaya et al., 2016; Zakharova et al., 2012). Analogous experimental procedures were carried out for various aliquots of concentrated surfactant solution. A series of surfactant stock solutions with different concentrations were prepared in such a way that the maximum dilution of oligonucleotide-EB complex didn't exceed 10% upon surfactant solution addition. Each of concentration dependences was performed twice, and the standard deviation of results was less than 2%. The following equation was used for the quantitative estimation of the binding degree of ONu to amphiphile:

$$\beta = \frac{(I_{bound} - I_{obs})}{I_{bound} - I_{free}} \quad (1)$$

where I_{free} and I_{bound} are the intensities of fluorescence of free EB and probe bound to ONu, I_{obs} is the intensity observed in the titration measurements at certain amount of amphiphile added.

Registration of fluorescence spectra of amphiphile/BSA binary systems was carried out at 25 °C and excitation wavelength of 280 nm. Emission spectra were registered in the range of 290–450 nm and with scanning speed of 120 nm/min. Quartz cuvettes with 1 cm width were used for fluorescence measurements. Synchronous fluorescence spectra were registered in the range of 200–400 nm at certain difference between excitation and emission wavelength (Δλ): Δλ = 20 nm and Δλ = 60 nm.

2.2.3. Dynamic and electrophoretic light scattering

Measurements of size and charge characteristics of samples were carried out using dynamic and electrophoretic light scattering techniques on a Malvern ZetaSizer Nano (Malvern Instruments Ltd., UK). Radiation source was He-Ne gas laser with 4 MW power and operating wavelength of 632.8 nm. Signals collected were treated in terms of frequency and phase analysis of scattered light using software attached to the device. All measurements were performed at scattering angle of 173°. Particle size calculation was performed in accordance with Stokes-Einstein equation (Eq. (2)).

$$D = \frac{kT}{6\pi\eta R} \quad (2)$$

where *k* is Boltzmann's constant, *T* is absolute temperature, η is the solvent's viscosity, *R* is hydrodynamic radius.

2.2.4. Turbidimetry

Phase transitions in amphiphile/DPPC mixtures were investigated by a Specord 250 PLUS spectrophotometer (Analytik Jena). Optical density versus temperature plot at 350 nm wavelength was registered for establishment of lipid main phase transition in surfactant/DPPC binary system. The temperature was varied in the range of 35–45 °C. Primarily turbidimetric plot for individual DPPC liposomes (0.7 mM) was obtained. Further amphiphile solutions were added to liposomes dispersions and analogous turbidimetric plot was registered. These operations were repeated for all surfactant/DPPC molar ratios. The turbidimetric plots were fitted to Van't Hoff two state models, which assumes that the inflection point in the turbidimetric plot obtained corresponds to the main phase transition of DPPC (Brand and Eglinton, 1965).

2.2.5. Release of metronidazole in vitro

Screening of metronidazole release from DPPC liposomes was performed using a Specord PLUS 250 (Analytik Jena) spectrophotometer. Dispersion of liposomes after preparation was purified from unencapsulated cargo using Amicon Ultra-0.5 mL centrifugal filters (MWCO 100 kDa) and centrifugation at 13 000 rpm during 10 min. Liposomes were diluted to 0.7 mM concentration of lipid and loaded to dialysis bag with 2–4 kDa pores. Dialysis was carried out in 100 mL of water. Aliquots of external water (1 mL) were withdrawn after equal time intervals and analyzed using spectrophotometer. Quantitative estimation of metronidazole amount in collected aliquot was carried out using absorbance at 319 nm (absorption maximum of metronidazole) and well-known extinction coefficient of metronidazole (11,000 M^{-1} cm^{-1}).

2.2.6. Fluorescence microscopy

To localize the oligonucleotide, the Hoechst 33342 dye (0.1 mg / ml) was added to samples of M-Hela cancer cell lines without and with IA-16(OH)/ONu lipoplexes (in the second case concentration of ONu was 1 mM, concentration of IA-16(OH) was 0.09 mM). The survey was carried out using a Nikon Eclipse Ci-S fluorescence microscope (Nikon, Japan) at a magnification of 1000× and by means of the multifunctional Cytell Cell Imaging system (GE Health Care Life Science, Sweden) using the Automated Imaging BioApp at a magnification of 100×.

3. Results and discussion

3.1. Aggregation behavior

Since functional activity of surfactants depends on their aggregation characteristics, at the first step of work the critical micelle concentration (cmc) values were determined for three amphiphiles studied by tensiometry technique. The surfactant concentration, at which the inflection is observed in surface tension–amphiphile molar concentration plot, was taken as cmc (Fig. 2). It could be seen that like in the case of conventional analogues of ammonium series, the trend of cmc decrease with increase of the length of hydrophobic tail is observed. It should be noted that elongation of alkyl tail by 2 carbon atoms leads to

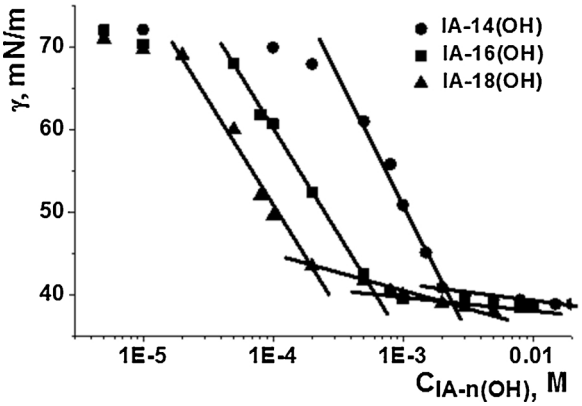

Fig. 2. Surface tension isotherms for IA-n(OH) aqueous solutions (n = 14,16,18); 25 °C.

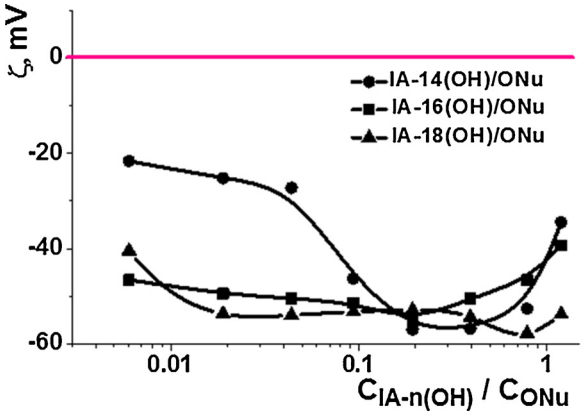

Fig. 4. Electrokinetic potential versus surfactant/ONu molar ratio for IA-n (OH)/ONu binary systems; 25 °C.

approximate 3-fold decrease of cmc value. The cmc values found are 2 mM for IA-14(OH), 0.6 mM for IA-16(OH) and 0.2 mM in the case of IA-18(OH). Noteworthy, the aggregation thresholds of amphiphiles bearing hydroxyethyl fragment are slightly lower than imidazolium-containing surfactants without hydroxyl groups (Samarkina et al., 2017a) that is due to the contribution of H-bonds of hydroxyl groups to aggregate formation.

3.2. Interaction with DNA decamer

One of the most important directions of surfactant application, including amphiphiles bearing natural fragment, is fabrication of promising systems for gene delivery purposes (so-called nonviral vectors). Principal disadvantage of this type of carriers is low gene expression efficiency in comparison with viral counterparts (Zabner et al., 1995). This fact stimulates the search of novel nonviral vectors and the estimation of role of different factors (hydrophobic, electrostatic and π-π-stacking interactions, hydrogen bonding, etc.) in variation of complexation ability of surfactant/DNA binary systems.

From physico-chemical point of view, the main characteristics of potential carriers of nucleic acids are the size of surfactant/DNA complex, its charge, as well as binding degree of components. Therefore, dynamic and electrophoretic light scattering and fluorescence spectroscopy techniques were applied for evaluation of potential capability of the series of hydroxyethylated imidazolium-containing amphiphiles to act as nonviral vectors for model oligonucleotide (ONu).

Using dynamic light scattering the aggregate size fabricated in IA-n (OH)/ONu binary systems were determined (Fig. 3 and S1). In all three cases the binding between components is implemented beginning with

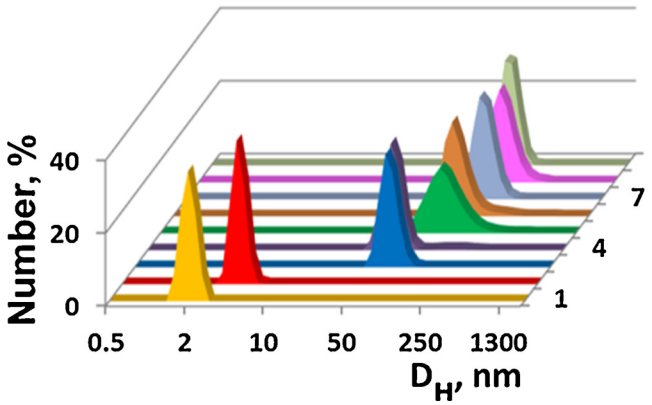

Fig. 3. Number-averaged size distribution for IA-14(OH)/ONu binary systems at surfactant/ONu various molar ratios: 1 – individual ONu, 2 – 0.006, 3 – 0.02, 4 – 0.044, 5 – 0.094, 6 – 0.194, 7 – 0.394, 8 – 0.79; 9 – 1.2; 25 °C.

minimal surfactant/DNA molar ratios that is evidenced by the increase of aggregates size from 2 nm to 50 nm and higher upon increasing of surfactant concentration. Remarkably enough, the hydrodynamic diameter of lipoplexes formed is less or equal to 250 nm. In accordance with long-held belief, this provides the prolonged circulation of lipoplex in blood stream (Hunt et al., 2007). It is noteworthy, that fabricated lipoplexes have suitable sustainability and their size characteristics could be reproduced after 5 days of storage, which was depicted in Fig. S2 in terms of examination of hydrodynamic diameter of IA-14(OH)/ONu binary system. The observed bimodal size distribution at the fifth day testifies the initiation of destruction of lipoplexes agglomeration of particles.

The next valuable requirement for potential nonviral vector is capability to electrostatic binding with nucleotide units, which results in compaction of DNA macromolecule and facilitates lipoplex permeation through cell membrane. To evaluate the role of electrostatic binding with IA-n(OH), an electrophoretic titration of ONu solution by surfactant solutions were performed (Fig. 4). It could be seen that in all cases an addition of surfactant is unable to compensate negative charge of phosphate groups of DNA decamer: corresponding zeta potential values for three IA-n(OH)/ONu binary systems studied are less or equal to −20 mV regardless of the amount of surfactant added. This phenomenon observed could be due to several reasons. Firstly, a positive charge of surfactant head group is delocalized by imidazolium ring and the absence of point charge focused on one atom doesn't allow to neutralize ONu charge. Secondly, a bulky head group is capable to interrupt the binding of imidazolium-containing amphiphiles with ONu, complicating localization of head groups in the area of DNA decamer phosphate groups. The behavior found is unconventional for cationic surfactants, since the main mechanism of interaction between cationic amphiphiles and nucleic acids is electrostatic attraction, as it was described earlier (Gabdrakhmanov et al., 2015b; Zakharova et al., 2012). However, analogous effect was previously observed in our works for imidazolium-containing amphiphiles without OH-groups (Samarkina et al., 2017a), which attests to the key role of the nature of surfactant head group in formation of complexes with nucleotides.

Quantitative estimation of IA-n(OH) binding ability toward ONu was performed using fluorescent assay of ethidium bromide (EB) exclusion. This technique is based on the capability of foreign additives, in particular cationic amphiphiles IA-n(OH), to exclude this fluorescent probe from EB/ONu complexes accompanying by the quenching of fluorescence intensity (Fig. S3). The fluorescence spectra registered for EB/ONu in the presence of various amounts of IA-n(OH) amphiphile series were used for further evaluation of the degree of binding between ONu and imidazolium-containing amphiphiles bearing hydroxyethyl groups in accordance with Eq. (1) (Fig. 5). β values calculated for all homologues studied reach 95% that is close to value for imidazolium-

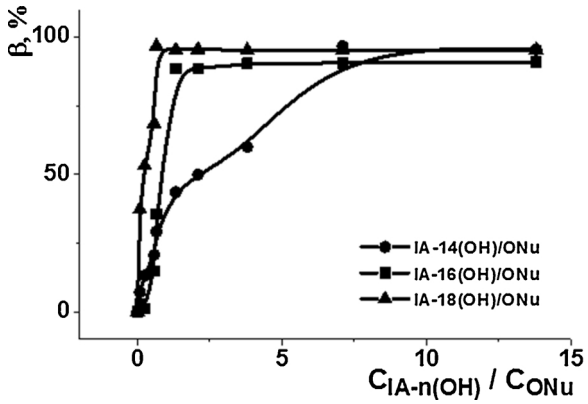

Fig. 5. Degree binding of IA-n(OH) with ONu versus surfactant/ONu molar ratio plot for IA-n(OH)/ONu binary systems.

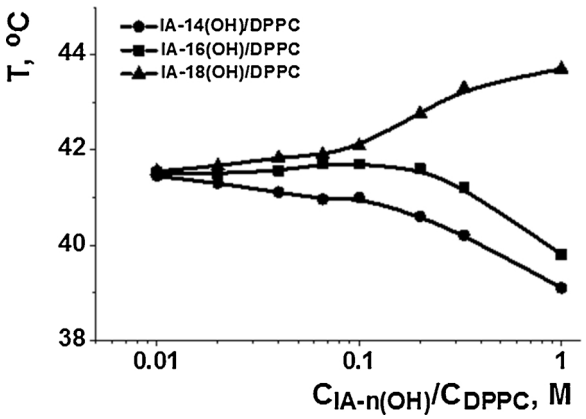

Fig. 6. Temperature of DPPC main phase transition versus surfactant/lipid molar ratio for IA-n(OH)/DPPC binary systems.

containing amphiphiles without OH-groups (Samarkina et al., 2017a). An elongation of amphiphile hydrophobic tail reduces surfactant concentration corresponding to achievement of maximal binding degree. Therefore, high contribution of hydrophobic interactions to complexation of imidazolium-containing amphiphiles bearing OH-groups with ONu becomes obvious. Besides, the realization of unconventional intercalation mechanism of binding could be proposed. This mechanism of binding corresponds to integration of plain imidazolium head groups between nucleotide nitrogenous bases. However, the presence of hydroxyethyl fragment in amphiphile molecule slightly decreases this capability of binding, because the β values achieve 100% in the case of imidazolium-containing amphiphiles without OH-groups (Samarkina et al., 2017a). Interestingly, in earlier reported investigations of ionic liquids, the derivatives of imidazolium showed inability to interact between nitrogenous bases in the absence of long-chained alkyl tail in the structure (Jumbri et al., 2016). This means that in our case an involvement of two contributions to binding takes place: hydrophobic interactions and intercalation integration lead to the almost quantitative binding between amphiphile and DNA decamer even in conditions of low contribution of conventional electrostatic binding of components.

3.3. Membranotropic properties

The next important characteristics of amphiphiles as agents for gene delivery is their capability to penetrate through cell wall barrier, mainly consisting of lipid bilayer. In vitro these processes could be simulated using model liposomes constructed from DPPC molecules and investigated through turbidimetry. This technique is based on the evaluation of DPPC main phase transition temperature in the presence of varied amount of surfactant. Usually the main gel–liquid-crystal phase transition temperature (T_{PT}) in DPPC equals to 41 ± 0.5 °C (Fig. S4), corresponding to the inflection point in turbidimetric plot, and the modified additives like surfactants are capable to change this temperature.

The results obtained for various surfactant/lipid molar ratio in the case of IA-n(OH) homologous series are present in Fig. 6 as $T_{PT} = f[C_{IA\text{-}n(OH)}/C_{DPPC})]$ and provided sufficient evidence to establish that the effects observed strongly depends on the length of hydrophobic tail. In the cases of IA-14(OH) and IA-16(OH) a decrease of T_{PT} value with increase of surfactant/lipid molar ratio indicates an integration of molecules of these amphiphiles into lipid bilayer. It leads to the loosening of lipid molecule packing facilitating their transition to liquid crystalline form. This phenomenon may provide the increase of lipid bilayer permeability that could be used in biotechnologies for transport of drugs and genetic material through the cell wall. Oppositely, in the case of the higher homologue IA-18(OH) $\Delta T_{PT} > 0$ that is unconventional result and could be the evidence of stabilization of DPPC lipid bilayer. This result could be due to several reasons: (i) increase of partition coefficient of surfactant in gel phase in comparison with bulk phase; (ii) approximation and coincidence of the length of hydrophobic tail of surfactant molecule to DPPC molecule, leading to increase of packing density of hydrophobic tails in lipid bilayer.

It could be speculated that the difference in the influence of lower and highest homologues on T_{PT} value is due to the fact that only in the case of IA-18(OH) alkyl tails are longer compared to DPPC tails. This makes it possible to rich them for the inner layer and bridging both layers, which would limit mobility of surfactant molecules and increase the ordering of the whole system. It is most likely, that this effect is cumulative and appears only at $C_{IA\text{-}18(OH)}/C_{DPPC} \geq 0.1$, when the contribution of additional interactions becomes sufficient to decrease the fluidity of DPPC liposomes.

It should be noted, that in the case of reported earlier non-hydroxyethylated amphiphiles with the same length of hydrophobic tail (Samarkina et al., 2017a) a similar trend was observed. This supports the validity of the mentioned hypothesis. Interestingly, disordering effect of tetradecyl and hexadecyl derivatives of two types of amphiphiles in terms of ΔT_{PT} values are close, while stabilization effect for octadecyl derivatives is significantly higher for non-functionalized analog. This effect could be explained in terms of the fact that IA-18(OH) has more bulky head group, which interrupts the tighter packing of molecules in lipid bilayer and competes with abovementioned stabilizing effect of interactions with the inner layer of lipid.

The observed significant differences in membranotropic properties of IA-n(OH) amphiphiles require more detailed investigation, especially at equimolar ratios of components demonstrating maximal divergence for various homologues. In particular, the structure of particles formed in these three cases is of interest, which was examined using dynamic light scattering technique above the T_{PT} value. As could be seen from Fig. 7, the length of hydrophobic tail of IA-n(OH) has no effect on the structure of DPPC particles, i.e. D_H value is constant in all cases (~ 100 nm) and polydispersity index of the systems is less or equal to 0.1. This testifies to the maintenance of closed bilayer structure of liposomes in IA-n(OH)/DPPC binary systems.

Therefore, a variation in the length of hydrophobic tail in the series of imidazolium-containing amphiphiles allows to initiate disordering and the compression of lipid bilayer, thereby changing the membrane permeability while leaving undestroyed the structure of lipid bilayer.

This conclusion about correlation between disordering effect of amphiphiles and increase in permeability may be discussed in terms of release of hydrophilic drug metronidazole from DPPC based liposomes. As documented earlier (Kuznetsova et al., 2019a) the liposomal formulation modified with unsubstituted imidazolium surfactants bearing tetradecyl tail (IA-14) exhibiting same disordering effect on lipid bilayer provide prolong release of cargo molecules compared to free drug.

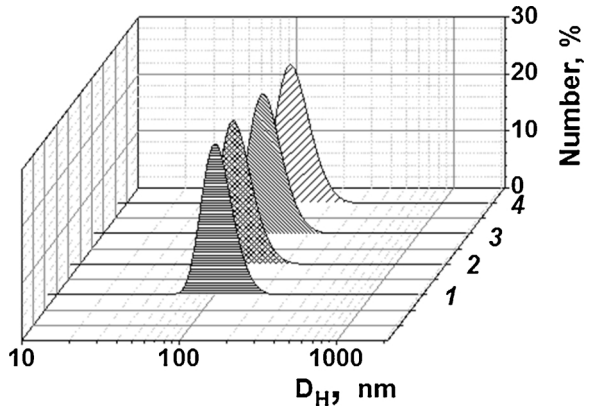

Fig. 7. Number-averaged size distribution for IA-n(OH)/DPPC binary mixtures at equimolar ratios of components: 1) individual DPPC liposomes, 2) IA-14(OH)/DPPC; 3) IA-16(OH)/DPPC; 4) IA-18(OH)/DPPC; 45 °C.

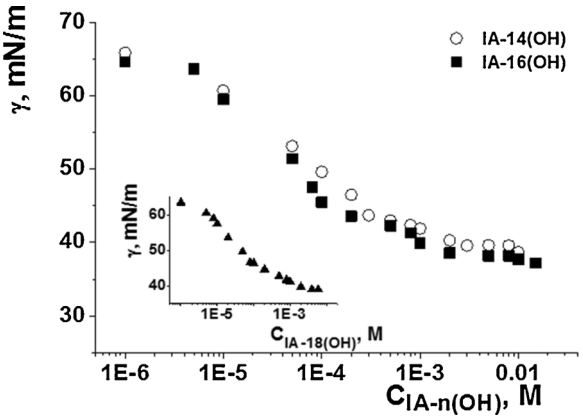

Fig. 9. Surface tension isotherms for IA-n(OH)/BSA binary systems at the fixed surfactant concentration (0.05% w/w); 25 °C.

Meanwhile, the comparison of metronidazole release from individual DPPC liposomes and liposomes modified with IA-14 (Fig. S5) testified that a greater amount of cargo is released at the same time. Consequently, it could be concluded, that the leakage of entrapped compound from liposomes containing amphiphile capable to disorder lipid bilayer is higher, than individual liposomes. It is equivalent to the increased permeability of the former liposome and confirm abovementioned hypothesis.

Taking into account membranotropic activity of imidazolium surfactants revealed, an ability of lipoplexes to cross cell membrane was tested by fluorescent microscopy. Corresponding experiments were carried out on the example of hexadecyl derivative of IA-n(OH) and M-Hela cancel cells. Localization of lipoplex in the cell was visualized using Hoechst 33342 dye capable to bind with nucleotides containing adenine and thymine nitrogen bases. Therefore, it could color both DNA of tumorous cells located in the nucleus and oligonucleotide as a part of IA-16(OH)/ONu lipoplexes. Collected data for M-Hela cells in the absence and in the presence of lipoplex (Fig. 8) allows to clearly reveal a localization of ONu bound to IA-16(OH) within M-Hela cells cytoplasm. This fact is the evidence of lipoplex penetration through the cell membrane.

3.4. Interaction with bovine serum albumin

Currently, the change of protein conformation is one of the most important problems, since the onset and progression of many human diseases may be involved on this process [43]. Therefore, the problem of peptide structure stabilization is challenging task. Promising way is the application of amphiphilic compounds for this purpose; however in some cases protein denaturation processes is possible [17]. For this reason, an establishment of the dependence of surfactant chemical structure on conformational behavior of protein macromolecules requires additional investigations. An often-used macromolecule is the bovine serum albumin (BSA) consisting of 583 amino acid residues (molecular weight is 66.5 kDa) and that follows the structure of the main transport protein of blood, human serum albumin. In the framework of this investigation the protein/surfactant interactions were examined through complexation of BSA with the series of IA-n(OH) amphiphiles. To evaluate surfactant structure effect all experiments were carried out at fixed BSA concentration (0.05 mass. %) and varied concentration of amphiphile.

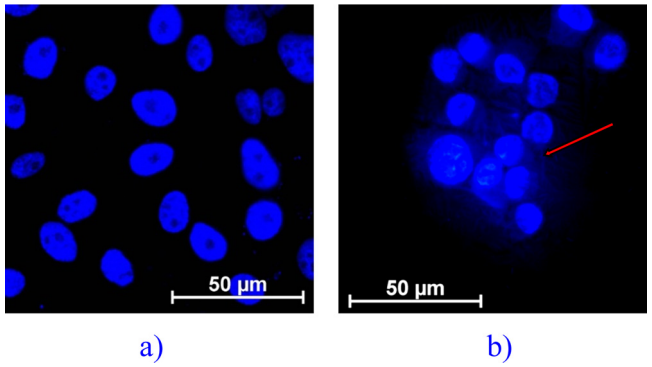

Fig. 8. Fluorescent micrographs of M-Hela cells in the absence (a) and in the presence of IA-16(OH)/ONu lipoplex (b, C_{ONu} = 1 mM, $C_{IA\text{-}16(OH)}$ = 0.09 mM). Arrows indicate the presence of oligonucleotide in the cytoplasm of cells.

the aggregation characteristics of surfactant/BSA system were evaluated (Fig. 9, S6) using tensiometry technique. There are two inflection points in the corresponding isotherms of surface tension for IA-n(OH)/BSA binary systems. The first one in the region of low surfactant concentrations reflects critical aggregation concentration (cac) indicating initiation of surfactant/BSA complexation. The second point in the region of high amphiphile concentrations is related to surfactant cmc value that denotes the BSA saturation by amphiphile molecules and the formation of free surfactant aggregates. The aggregation data obtained for all amphiphiles studied are given in Table 1.

Analysis of the values showed that in all three cases 10-25-fold decrease of aggregation threshold of two-component system in comparison with individual solutions was reached and transition from low to high homologue could additionally increase aggregation capability of the system by 5 times. It is the evidence of the crucial role of hydrophobic interactions between lipophilic tails of surfactants and hydrophobic pockets of peptide macromolecule.

The particle size distribution of the aggregates formed in IA-n(OH)/BSA solutions were analyzed by the dynamic light scattering (Figs. 10, S7). In all three cases within whole concentration range studied the hydrodynamic diameter values were constant (10–12 nm) and coincided with the size of individual BSA. This indicates that surfactant/BSA complexes are sustainable and amphiphile additives do not contribute significantly to polypeptide size. More detailed information

Table 1
Aggregation threshold values for IA-n(OH)/BSA binary systems and IA-n(OH) individual solutions determined by tensiometry technique.

n	IA-n(OH) / BSA		IA-n(OH)
	cac, mM	cmc, mM	cmc, mM
14	0.3	3	2
16	0.1	2.5	0.6
18	0.07	1.5	0.2

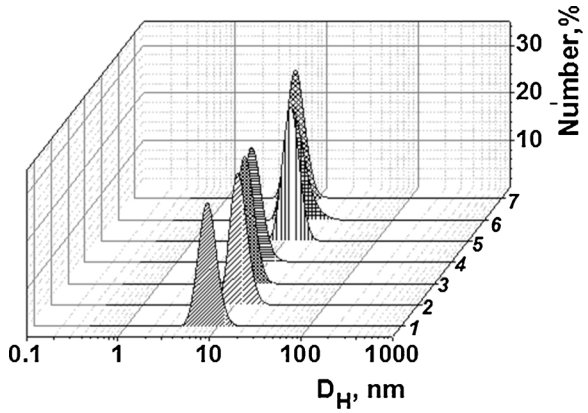

Fig. 10. Number-averaged size distribution for IA-14(OH)/BSA binary system for various surfactant concentrations: 1 – individual BSA, 0.05% mass., 2 – 0.001 mM, 3 – 0.01 mM, 4 – 0.1 mM, 5 – 1 mM, 6 – 5 mM, 7–10 mM); 25 °C.

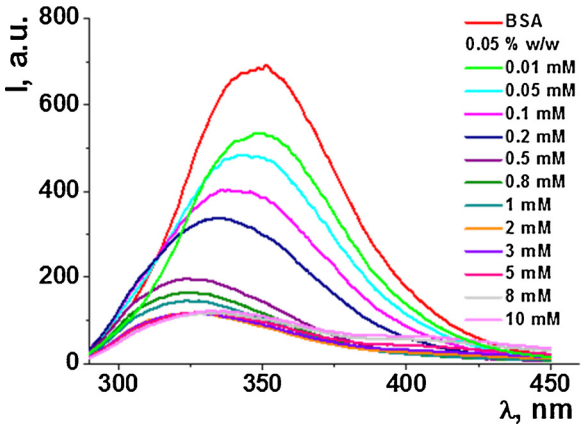

Fig. 12. Emission fluorescence spectra of IA-14(OH)/BSA binary systems for various surfactant concentration (BSA amount is constant and equals to 0.05% w/w); 25 °C.

could be obtained by the analysis of intensity-averaged size distribution. Fig. S8 shows the size characteristics for IA-14(OH)/BSA and IA-18(OH)/BSA samples. Noteworthy, there is the presence of large aggregates with D_H = 600–900 nm, indicating the slight partial denaturation of protein macromolecules with amphiphile addition. However, the capability to protein molecule unfolding was more pronounced (Gabdrakhmanov et al., 2018; Misra et al., 2015) up to coagulation processes occurring in the case of earlier studied amphiphiles bearing other head groups (Vasilieva et al., 2018a).

For estimation of charge characteristics in IA-n(OH)/BSA binary systems the electrophoretic light scattering technique was involved. Because BSA macromolecule has a negative charge, an addition of cationic surfactant makes it possible to expect component binding by electrostatic mechanism. The experimental data confirm this hypothesis, according which transition of zeta potential values from negative to positive region crossing the zero was observed with increase of surfactant concentration (Fig. 11). It should be noted that elongation of hydrophobic tail of imidazolium-containing amphiphiles has no effect on the reaching of isoelectric point: zero zeta potential values are observed at equal concentrations for all amphiphiles studied.

The next step of investigation includes evaluation of the interaction effectiveness of imidazolium-containing amphiphiles bearing OH-groups with BSA using various fluorescent techniques. Registration of intrinsic fluorescence emission spectra for IA-n(OH)/BSA binary systems allows to show that in all cases an addition of surfactant results not only in the quenching of fluorescence, but in hypsochromic shift (Figs. 12, S9). Phenomenon of BSA fluorescence decrease with

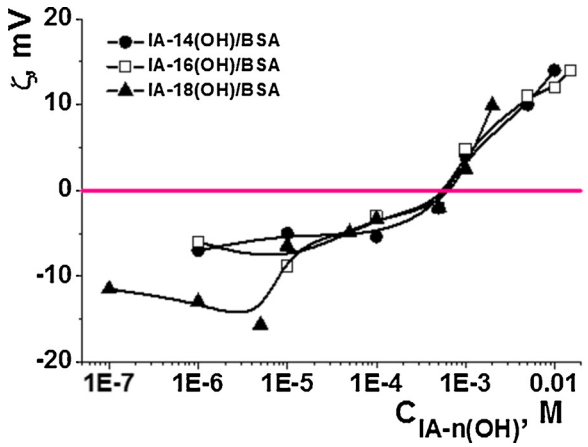

Fig. 11. Electrokinetic potential of IA-n(OH)/BSA binary systems versus amphiphile concentration plot (0.05 % w/w); 25 °C.

concentration of foreign additive is often observed for interactions of cationic surfactants and is the evidence of formation of the complex between polypeptide and IA-n(OH) amphiphiles. The binding between components changes polarity of microenvironment around binding sites of peptide macromolecule: a more hydrophobic microenvironment causes a blue shift of the emission maximum position.

There are three types of amino acid substitutions composing BSA: tyrosine (Tyr), tryptophan (Trp) and phenylalanine (Phe) (Janeka et al., 2017; Khan et al., 2018; Misra et al., 2015), among them a significant fluorescence contribution is made by only first two of them. The synchronous fluorescence technique was used seeking information on what amino acid residue (Tyr or Trp) participates in interaction with surfactant molecules. This method is based on measurements with fixed difference of excitation and emission wavelengths Δλ: Δλ = 20 nm reflecting binding by tyrosine residue and Δλ = 60 nm characterizing binding by tryptophan fragment. Figs. 13 and S10 show the synchronous fluorescence spectra for IA-14(OH)/BSA and IA-18(OH)/BSA binary systems. An evaluation of the contribution of each amino acid residue could be performed through the comparison of the influence of equal surfactant additives on capability to fluorescence quenching for synchronous spectra with Δλ = 20 nm and Δλ = 60 nm (as a percentage by initial maximal intensity value). Analysis of presented data for both homologues showed that the intensity of fluorescent band responsible for contribution of tryptophan fragment begin to reduce even at low amounts of surfactants added and its further reaches almost zero intensity. At the same time, an analogous fluorescent band for tyrosine for both surfactants examined varied in different ways. An increase of fluorescence occurs for IA-14(OH)/BSA binary system at low surfactant additives, which is the evidence of unfolding of protein macromolecule and the localization of tyrosine fragment at the interface with bulk. A fluorescence quenching was observed for IA-18(OH)/BSA binary system, but it took place after cac value reaching. Comparative evaluation of abovementioned results allows us to note that Trp fluorescent band quenching is more pronounced. Therefore, the binding between surfactant and BSA favorably occurs through Trp amino acid residue, and the interaction with Tyr moiety is less pronounced.

4. Conclusions

In summary the investigation of interaction of imidazolium-containing amphiphiles bearing hydroxyethyl fragment with various biomolecules (DNA decamer, model lipid bilayer and bovine serum albumin) was carried out using various physico-chemical methods. The transition from unsubstituted analogues to ones bearing hydroxyethyl fragment reduces aggregation thresholds by 1.5–2 times. Binding with DNA decamer proceeds almost quantitatively and lipoplexes obtained

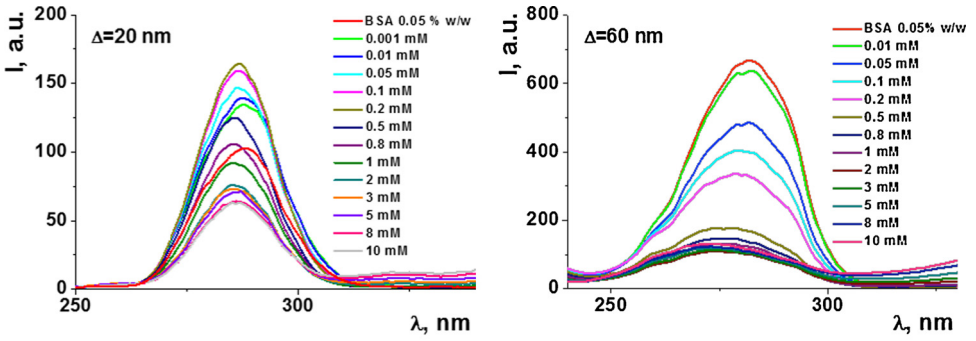

a) b)

Fig. 13. BSA synchronous fluorescence spectra in the presence of different amounts of surfactant for IA-14(OH)/BSA binary system, $\Delta\lambda = 20$ nm (a), $\Delta\lambda = 60$ nm (b), 25 °C.

could be recommended for further biological examination as candidates for perspective nonviral vectors. Unconventional mechanism of component binding was revealed involving intercalation and hydrophobic interactions. Variation of the length of hydrophobic tail of hydroxyethylated imidazolium-containing amphiphiles could be used as a tool for regulation of the permeability of model lipid bilayer. Transition of individual surfactant solutions to their mixtures with BSA is accompanied by 8-fold decrease of aggregation thresholds and characterized by the presence of two critical points. The favorable binding site of surfactant and BSA is tryptophan amino acid residue.

Acknowledgement

This work was financially supported by Russian Science Foundation (project № 19-73-30012).

Appendix A. Supplementary data

Supplementary material related to this article can be found, in the online version, at doi:https://doi.org/10.1016/j.chemphyslip.2019.104791.

References

Aggarwal, R., Singh, S., 2018. Synthesis, characterization and evaluation of surface and thermal properties of 3-cyclohexyloxy-2-hydroxypropyl pyridinium and imidazolium surface-active ionic liquids. J. Surfact. Deterg. 21, 43–52. https://doi.org/10.1002/jsde.12002.

Albalawi, A.H., El-Sayed, W.S., Aljuhani, A., Almutairi, S.M., Rezki, N., Aouad, M.R., Messali, M., 2018. Microwave-assisted synthesis of some potential bioactive imidazolium-based room-temperature ionic liquids. Molecules 23 (7), E1727. https://www.ncbi.nlm.nih.gov/pubmed/30011951.

Asadov, Z.H., Nasibova, Sh.M., Rahimov, R.A., Gasimov, E.K., Muradova, S.A., Rzayev, F.H., Asadova, N.Z., Zubkov, F.I., 2019. Effects of head group on the properties of cationic surfactants containing hydroxyethyl- and hydroxyisopropyl fragments. J. Mol. Liq. 274, 125–132. https://www.sciencedirect.com/science/article/pii/S0167732218335888.

Baker, G., Pandey, S., Baker, S., 2004. A new class of cationic surfactants inspired by N – alkyl – N – methyl pyrrolidinium ionic liquids. Analyst 129, 890–892. https://pubs.rsc.org/en/content/articlelanding/2004/an/b410301g#!divAbstract.

Benedetto, A., Ballone, P., 2016. Room temperature ionic liquids meet biomolecules: a microscopic view of structure and dynamics. ACS Sustainable Chem. Eng 4 (2), 392–412. https://doi.org/10.1021/acssuschemeng.5b01385.

Benedetto, A., 2017. Room-temperature ionic liquids meet bio-membranes: the state-of-the-art. Biophys. Rev. 9 (4), 309–320. https://www.ncbi.nlm.nih.gov/pubmed/28779453.

Benedetto, A., Ballone, P., 2018. Room-temperature ionic liquids and biomembranes: setting the stage for applications in pharmacology, biomedicine, and bionanotechnology. Langmuir 34 (33), 9579–9597. https://doi.org/10.1021/acs.langmuir.7b04361.

Bombelli, C., Bordi, F., Ferro, S., Giansanti, L., Jori, G., Mancini, G., Mazzuca, C., Monti, D., Ricchelli, F., Sennato, S., Venanzi, M., 2010. New cationic liposomes as vehicles of m-tetrahydroxyphenylchlorin in photodynamic therapy of infectious diseases. Mol. Pharm. 5, 672–679. https://doi.org/10.1021/mp800037d.

Brand, J.C.D., Eglinton, G., 1965. Applications of Spectroscopy to Organic Chemistry. Oldbourne Press, London.

Chauhan, V., Singh, S., Kamboj, R., Mishra, R., Kaur, G., 2014. Synthesis, micellization properties, and cytotoxicity trends of N-hydroxyethyl-3-alkyloxypyridinium surfactants. Colloid Polym. Sci. 292, 467–476. https://link.springer.com/article/10.1007/s00396-013-3083-x.

Demberelnyamba, D., Kim, K.-S., Choi, S., Park, S.-Y., Lee, H., Kim, Ch.-J., Yoo, I.-D., 2004. Synthesis and antimicrobial properties of imidazolium and pyrrolidinonium salts. Bioorg. Med. Chem. 12, 853–857. http://europepmc.org/abstract/MED/14980596.

Gabdrakhmanov, D.R., Samarkina, D.A., Semenov, V.E., Krylova, E.S., Reznik, V.S., Zakharova, L.Ya., 2016a. Cationic surfactant with 1,2,4-triazole- and uracil moieties as amphiphilic building blocks for supramolecular nanocontainers. J. Mol. Liq. 218, 255–259. https://www.sciencedirect.com/science/article/pii/S0167732215307807.

Gabdrakhamanov, D.R., Samarkina, D.A., Semenov, V.E., Saifina, L.F., Valeeva, F.G., Reznik, V.S., Zakharova, L.Ya., 2016b. Substrate specific nanoreactors based on pyrimidine-containing amphiphiles of various structures for cleavage of phosphonates. Phosphorus Sulfur Silicon Relat. Elem. 191, 1673–1675. https://doi.org/10.1080/10426507.2016.1227820.

Gabdrakhmanov, D., Samarkina, D., Semenov, V., Syakaev, V., Giniyatullin, R., Gogoleva, N., Reznik, V., Latypov, Sh., Konovalov, A., Pokrovsky, A., Zuev, Y., Zakharova, L., 2015a. Novel dicationic pyrimidinic surfactant: self-assembly and DNA complexation. Colloids Surf. A 480, 113–121.

Gabdrakhmanov, D.R., Samarkina, D.A., Valeeva, F.G., Saifina, L.F., Semenov, V.E., Reznik, V.S., Zakharova, L.Y., Konovalov, A.I., 2015b. Supramolecular systems based on dicationic pyrimidine-containing surfactants and polyethyleneimine. Russ. Chem. Bull 64, 573–578. https://link.springer.com/article/10.1007/s11172-015-0902-x.

Gabdrakhmanov, D.R., Valeeva, F.G., Samarkina, D.A., Lukashenko, S.S., Mirgorodskaya, A.B., Zakharova, L.Ya., 2018. The first representative of cationic amphiphiles bearing three unsaturated moieties: self-assembly and interaction with polypeptide. Colloids Surf. A 558, 463–469. https://www.sciencedirect.com/science/article/pii/S0927775718309932.

Gabdrakhmanov, D.R., Valeeva, F.G., Semenov, V.E., Samarkina, D.A., Mikhailov, A.S., Reznik, V.S., Zakharova, L.Y., 2016c. Supramolecular catalysts based on novel pyrimidinophane: influence of additives of polymer and lanthanum ions. Macroheterocycles 9 (1), 29–33.

Hunt, K.K., Vorburger, S.A., Swisher, S.G., 2007. Gene Therapy for Cancer. Humana Press, New Jersey.

Janeka, T., Czy´znikowska, Z., Łuczy´nski, J., Gudi˜na, Ed.J., Rodrigues, L.R., Gał ezowska, J., 2017. Physicochemical study of biomolecular interactions between lysosomotropic surfactants and bovine serum albumin. Colloids Surf. B 159, 750–758. https://www.ncbi.nlm.nih.gov/pubmed/28886512.

Jumbri, K., Ahmad, H., Abdulmalek, E., Basyaruddin, M., Rahman, A., 2016. Binding energy and biophysical properties of ionic liquid-DNA complex: understanding the role of hydrophobic interactions. J. Mol. Liq. 223, 1197–1203. https://www.sciencedirect.com/science/article/pii/S0167732216315549.

Kashapov, R.R., Razuvayeva, Yu.S., Ziganshina, A.Y., Mukhitova, R.K., Sapunova, A.S., Voloshina, A.D., Zakharova, L.Ya, 2019. Self-assembling and biological properties of single-chain dicationic pyridinium-based surfactants. Colloids Surf. B 175, 351–357. https://www.sciencedirect.com/science/article/pii/S0927776518308907.

Kaur, M., Singh, G., Kumar, S., Tejwant, N., Kang, S., 2018. Thermally stable microemulsions comprising imidazolium based surface active ionic liquids, non-polar ionic liquid and ethylene glycol as polar phase. J. Colloid Interface Sci. 511, 344–354. https://macroheterocycles.isuct.ru/en/system/files/mhc151194g_0.pdf. https://www.sciencedirect.com/science/article/pii/S0021979717311839.

Khan, M.V., Zakariya, S.M., Khan, R.H., 2018. Protein folding, misfolding and aggregation: a tale of constructive to destructive assembly. Int. J. Biol. Macromol. 112, 217–229. https://www.sciencedirect.com/science/article/pii/S014181301734415X.

Koirala, S., Roy, B., Guha, P., Bhattarai, R., Sapkota, M., Nahak, P., Karmakar, G., Mandal, A.K., Kumar, A., Panda, A.K., 2016. Effect of double tailed cationic surfactants on the physicochemical behavior of hybrid vesicles. RSC Adv. 6, 13786–13796. https://pubs.rsc.org/en/content/articlelanding/2016/ra/c5ra17774j#!divAbstract.

Kumar, S., Scheidt, H.A., Kaur, N., Kaur, A., Kang, T.S., Huster, D., Mithu, V.S., 2018. Amphiphilic ionic liquid-induced membrane permeabilization: binding is not enough.

J. Phys. Chem. B 122, 6763–6770. https://doi.org/10.1021/acs.jpcb.8b03733.
Kumar Majeti, B., Sunil Singh, R., Kumar Yadav, S., Reddy Bathula, S., Ramakrishna, S., Vamanrao Diwan, P., Sakunthala Madhavendra, S., Chaudhuri, A., 2004. Enhanced intravenous transgene expression in mouse lung using cyclic-head cationic lipids. Chem. Biol. 11, 427–437. https://www.cell.com/fulltext/S1074-5521(04)00087-0.
Kuznetsova, D.A., Gabdrakhmanov, D.R., Lukashenko, S.S., Ahtamyanova, L.R., Nizameev, I.R., Kadirov, M.K., Zakharova, L.Ya, 2019a. Novel hybrid liposomal formulations based on imidazolium-containing amphiphiles for drug encapsulation. Colloids Surf. B 178, 352–357. https://www.ncbi.nlm.nih.gov/pubmed/30901595.
Kuznetsova, D.A., Gabdrakhmanov, D.R., Lukashenko, S.S., Voloshina, A.D., Sapunova, A.S., Kulik, N.V., Nizameev, I.R., Kadirov, M.K., Kashapov, R.R., Zakharova, L.Ya., 2019b. Supramolecular systems based on cationic imidazole-containing amphiphiles bearing hydroxyethyl fragment: aggregation properties and functional activity. J. Mol. Liq. 289, 111058. https://doi.org/10.1016/j.molliq.2019.111058.
Lim, G.S., Jaenicke, S., Klähn, M., 2015. How the spontaneous insertion of amphiphilic imidazolium-based cations changes biological membranes: a molecular simulation study. Phys. Chem. Chem. Phys. 17, 29171–29183. https://pubs.rsc.org/ru/content/articlehtml/2015/cp/c5cp04806k.
Liu, H., Hu, J., Zhou, X., Liu, D., Xu, B., Zhou, Y., 2015. Synthesis, corrosion inhibition performance and biodegradability of novel alkyl hydroxyethyl imidazoline salts. J. Surf. Deterg. 18, 1025–1031. https://link.springer.com/article/10.1007/s11743-015-1725-3.
Mandal, S., Kuchlyan, J., Ghosh, S., Banerjee, C., Kundu, N., Banik, D., Sarkar, N., 2014. Vesicles formed in aqueous mixtures of cholesterol and imidazolium surface active ionic liquid: a comparison with common cationic surfactant by water dynamics. J. Phys. Chem. B 118, 5913–5923. https://doi.org/10.1021/jp501033n.
Mirgorodskaya, A.B., Kushnazarova, R.A., Zhukova, N.A., Mamedov, V.A., Zakharova, L.Ya., Sinyashin, O.G., 2018. Solubilization of biologically active heterocyclic compounds by biocompatible microemulsions. Russ. J. Phys. Chem. A 92 (12), 2588–2592. https://link.springer.com/article/10.1134/S0036024418120312.
Mirgorodskaya, A.B., Mamedov, V.A., Zakharova, L.Ya., Valeeva, F.G., Mamedova, V.L., Galimullina, V.R., Kushnasarova, R.A., Sinyashin, O.G., 2017. Surfactant solutions for enhancing solubility of new arylquinolin-2-ones. J. Mol. Liq. 242, 732–738. https://www.sciencedirect.com/science/article/pii/S0167732217322663.
Mirgorodskaya, A.B., Yackevich, E.I., Gabdrakhmanov, D.R., Lukashenko, S.S., Zuev, Yu.F., Zakharova, L.Ya, 2016. Self−organization and lipoplex formation of cationic surfactants with morpholinium head group. J. Mol. Liq. 220, 992–998. https://www.infona.pl/resource/bwmeta1.element.elsevier-d3ce1df3-ae72-38df-a81c-204c0e147d02.
Misra, P.K., Dash, U., Maharan, S., 2015. Investigation of bovine serum albumin-surfactant aggregation and physicochemical characteristics. Colloids Surf. A 483, 36–44. https://www.sciencedirect.com/science/article/pii/S0927775715300777.
Nandi, S., Bhattacharyya, K., 2018. Ionic liquid: complexity in structure and dynamics, interaction with proteins and in situ generation of metal nano-clusters for live cell imaging. Proc. Natl. Acad. Sci., India, Sect. A. 88 (3), 425–430. https://link.springer.com/article/10.1007%2Fs40010-018-0516-4.
Parray, M., Mir, M.H., Dohare, N., Maurya, N., Khan, A.B., Borse, M.S., Patel, R., 2018. Effect of cationic gemini surfactant and its monomeric counterpart on the conformational stability and esterase activity of human serum albumin. J. Mol. Liq. 260, 65–77. https://www.sciencedirect.com/science/article/pii/S0167732218305324.
Pashirova, T.N., Braïki, A., Zueva, I.V., Petrov, K.A., Babaev, V.M., Burilova, E.A., Samarkina, D.A., Rizvanov, I.Kh., Souto, E.B., Jean, L., Renard, P.-Y., Masson, P., Zakharova, L.Ya., Sinyashin, O.G., 2018. Combination delivery of two oxime-loaded lipid nanoparticles: time-dependent additive action for prolonged rat brain protection. J. Control. Release 290, 102–111. https://www.sciencedirect.com/science/article/pii/S0168365918305819.
Qin, M., Yin, T., Wang, S., Shen, W., 2015. Spectroscopic investigation on the interactions between cationic surfactants and bovine serum albumin. J. Dispersion Sci. Technol. 36, 1282–1289. https://doi.org/10.1080/01932691.2014.973031.
Samarkina, D.A., Gabdrakhmanov, D.R., Lukashenko, S.S., Khamatgalimov, A.R., Kovalenko, V.I., Zakharova, L.Y., 2017a. Cationic amphiphiles bearing imidazole fragment: from aggregation properties to potential in biotechnologies. Colloids Surf. A 529, 990–997. https://www.sciencedirect.com/science/article/pii/S0927775717306672.
Samarkina, D.A., Gabdrakhmanov, D.R., Lukashenko, S.S., Khamatgalimov, A.R., Zakharova, L.Y., 2017b. Aggregation capacity and complexation properties of a system based on an imidazole-containing amphiphile and bovine serum albumin. Russ. J. Gen. Chem. 87 (12), 2826–2831. https://link.springer.com/article/10.1134/S1070363217120118.
Samarkina, D.A., Gabdrakhmanov, D.R., Lukashenko, S.S., Nizameev, I.R., Kadirov, M.K., Zakharova, L.Ya, 2019. Homologous series of amphiphiles bearing imidazolium head group: complexation with bovine serum albumin. J. Mol. Liq. 275, 232–240. https://www.sciencedirect.com/science/article/pii/S016773221831763X.
Samarkina, D.A., Gabdrakhmanov, D.R., Semenov, V.E., Valeeva, F.G., Gubaidullina, L.M., Zakharova, L.Ya., Reznik, V.S., Konovalov, A.I., 2016. Self-assembling catalytic systems based on new amphiphile containing purine fragment, exhibiting substrate specificity in hydrolysis of phosphorus acids esters. Russ. J. Gen. Chem. 86 (3), 656–660. https://link.springer.com/article/10.1134/S1070363216030233.
Samarkina, D.A., Gabdrakhmanov, D.R., Semenov, V.E., Valeeva, F.G., Nikolaev, A.E., Saifina, L.F., Zakharova, L.Ya., 2017c. New amphiphilic multiheterocycle: micelle-forming properties and effect on the reactivity of phosphorus acid esters. Russ. J. Gen. Chem. 87 (9), 1977–1984. https://link.springer.com/article/10.1134/S1070363217090134.
Sinha, S., Tikariha, D., Lakra, J., Yadav, T., Kumari, S., Saha, S., Ghosh, K., 2016. Interaction of bovine serum albumin with cationic monomeric and dimeric surfactants: a comparative study. J. Mol. Liq. 218, 421–428. https://www.sciencedirect.com/science/article/pii/S0167732215313660.
Tateishi-Karimata, H., Sugimoto, N., 2018. Biological and nanotechnological applications using interactions between ionic liquids and nucleic acid. Biophys. Rev. 10 (3), 931–940. https://link.springer.com/article/10.1007%2Fs12551-018-0422-7.
Vasilieva, E.A., Lukashenko, S.S., Voloshina, A.D., Strobykina, A.S., Vasileva, L.A., Zakharova, L.Ya., 2018a. The synthesis and properties of homologous series of surfactants containing the pyrrolidinium head group with hydroxyethyl moiety. Russ. Chem. Bull. 67 (7), 1280–1286. https://app.dimensions.ai/details/publication/pub.1107353061?and_facet_journal=jour.1022309.
Vasilieva, E.A., Samarkina, D.A., Gaynanova, G.A., Lukashenko, S.S., Gabdrakhmanov, D.R., Zakharov, V.M., Vasileva, L.A., Zakharova, L.Ya, 2018b. Self-assembly of the mixed systems based on cationic surfactants and different types of polyanions: the influence of structural and concentration factors. J. Mol. Liq. 272, 892–901. https://www.sciencedirect.com/science/article/pii/S0167732218337437.
Wang, D., Galla, H.J., Drücker, P., 2018. Membrane interactions of ionic liquids and imidazolium salts. Biophys. Rev. 10 (3), 735–746. https://www.ncbi.nlm.nih.gov/pubmed/29302915.
Xie, H.-J., Liu, C.-C., Sun, Q., Fang, W.-J., 2016. The interactions between quaternary ammonium cationic surfactants and bovine serum albumin. Acta Phys. 32 (12), 2951–2960. http://www.whxb.pku.edu.cn/EN/10.3866/PKU.WHXB201609231.
Yackevich, E.I., Mirgorodskaya, A.B., Lukashenko, S.S., Zakharova, L.Ya., 2014. Polyfunctional supramolecular systems based on surfactants containing the hydroxyalkyl moiety in the head group. Russ. Chem. Bull. 63 (8), 1801–1806. https://link.springer.com/article/10.1007/s11172-014-0669-5.
Yan, Z., Dai, C., Zhao, M., Zhao, G., Li, Yu., Wu, X., Du, M., Liu, Y., 2015. pH−switchable wormlike micelle formation by N−alkyl−N−methylpyrrolidinium bromide−based cationic surfactant. Colloids Surf. A 482, 283–289. https://kundoc.com/pdf-ph-switchable-wormlike-micelle-formation-by-n-alkyl-n-methylpyrrolidinium-bromid.html.
Zabner, J., Fasbender, A.J., Moninger, T., Poellinger, K.A., Welsh, M.J., 1995. Cellular and molecular barriers to gene transfer by a cationic lipid. J. Biol. Chem. 270, 18997–19007. https://www.ncbi.nlm.nih.gov/pubmed/7642560.
Zakharova, L., Voronin, M., Semenov, V., Gabdrakhmanov, D., Syakaev, V., Gogolev, Y., Giniyatullin, R., Lukashenko, S., Reznik, V., Latypov, Sh., Konovalov, A., Zuev, Y., 2012. Supramolecular systems based on novel mono- and dicationic pyrimidinic amphiphiles and oligonucleotides: a self-organization and complexation study. ChemPhysChem 13, 788–796. https://www.ncbi.nlm.nih.gov/pubmed/22287323.
Zheng, L., He, Yi., Lin, P., Liu, L., Yang, H., Peng, Yi., Xie, Sh, 2017. Spectroscopic analysis of the interaction between tetra-(p-sulfoazophenyl-4-aminosulfonyl)-substituted aluminum(III) phthalocyanines and serum albumins. J. Innovative Opt. Health Sci. 10, 1650043–1650051. https://doi.org/10.1142/S1793545816500437.
Zheng, Zh., Xu, Q., Guo, J., Qin, J., Mao, H., Wang, B., Yan, F., 2016. Structure−antibacterial activity relationships of imidazolium-type ionic liquid monomers, poly(ionic liquids) and poly(ionic liquid) membranes: effect of alkyl chain length and cations. ACS Appl. Mater. Interfaces 8, 12684–12692. https://doi.org/10.1021/acsami.6b03391.
Zhou, T., Llizo, A., Li, P., Wang, Ch., Guo, Yu., Ao, M., Bai, L., 2013. High transfection efficiency of homogeneous DNA nanoparticles induced by imidazolium gemini surfactant as nonviral vector. J. Phys. Chem. C 117, 26573–26581. https://doi.org/10.1021/jp4061363. https://www.sciencedirect.com/science/article/pii/S0927775714008152.